

Simulation of Photoacoustic waves based Eigen-value and Eigen- function in Different Geometrical Resonance Cells

Naseem. Al-Mudfferi¹ , F. Yehya^{12*} , A. Masuadi¹ & Adnan Alsalmi¹

¹Department of Mathematics , Education Faculty, Albaydha University, Albaydha , Yemen

²Department of Physics, Faculty of Educational and sciences , Rada'a, Albaydha University, Albaydha , Yemen

*Corresponding author, Email: fahembajash@gmail.com

DOI: <https://doi.org/10.56807/buj.v2i2.49>

Abstract

We reported the simulation of photo acoustic signal which can be generated due to interaction between laser and molecules inside suitable designed cavities. We started with simulation of the eigenvalues and eigenfunctions acoustic waves generated in resonance cylindrical shape. The second step is done with rectangular box where we show that the eigenvalues and eigenvectors of acoustic wave have less efficiency than that from cylindrical. In addition, the effect of losses due to edges in the structure shape of rectangular has an extra reason to damping acoustic wave.

Keywords: Photoacoustic, cylinder, rectangular, eigenvalues, waves

محاكاة الموجات الضوء-صوتية المعتمدة على الدوال الذاتية في تجاويف رنانة هندسية مختلفة

الملخص

قمنا بعمل محاكاة للإشارة الضوء-صوتية الناتجة بسبب التفاعل بين الليزر والجزيئات داخل تجاويف مصممة بشكل مناسب. بدأنا بمحاكاة الموجات الصوتية ذات القيم الذاتية والدوال الذاتية المتولدة في الشكل الأسطواني الرنيني في الخطوة الثانية تمت الحسابات باستخدام صندوق مستطيل حيث لاحظنا أن كفاءة القيم الذاتية والمنحنيات الذاتية للموجة الصوتية أقل من تلك الموجودة في الأشكال الأسطوانية. بالإضافة إلى ذلك ، فإن تأثير الخسائر بسبب الحواف في شكل هيكل المستطيل له سبب إضافي لتثبيط الموجة الصوتية

الكلمات المفتاحية: ضوء-صوتية ، اسطوانة ، مستطيل ، قيم ذاتية ، موجات

Introduction:

Bessel's function is a famous partial differential equation. The solutions of Bessel equation have many applications in different fields. One of its applications help in determination the exact frequencies (Eigen value) and Eigen functions of light-sound interactions. In such interaction the light source is used to excite the molecules inside a resonance cavities to upper energy level E_2 . The excited molecule eventually falls down to its initial energy E through several processes as follow (Kreuzer-1971, Yehya-2011, Sigrist-1994):

- Radiation (stimulated or spontaneous emission of a photon),
- Chemical reactions such as a bond rearrangement-photochemistry
- Non-radiative deactivation, which consist in energy transfer towards surrounding molecules through collisions.

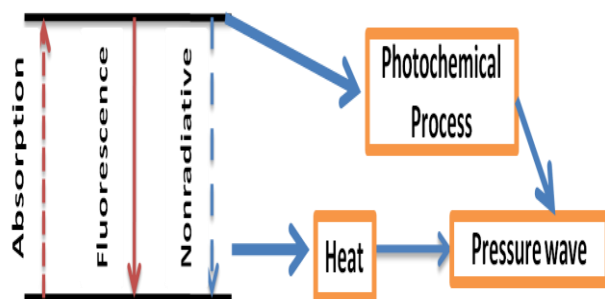


Fig-1: The physical mechanism of acoustic wave's generation

The third process is behind the increasing in a kinetic energy of the molecules which causes a local heating and subsequently a thermal expansion in the medium. If the intensity of light radiation is modulated at a given frequency, the induced periodical thermal expansion gives rise to a sound wave of the same frequency. This process takes the

name of Photoacoustic effect. (Bell-1880, Tyndall-1881, Rontgen-1881)

In Photoacoustic spectroscopy, the generated acoustic signal is fitting to a preamplifier and then to integrated system for amplification and converting the acoustic signal to an digital signal.

Theoretical background

1. Bessel equation (Tam-1983, Miklos-1989, Yehya & Chaudhary-2013)

The second order differential equation given as

$$x^2 y'' + xy' + (x^2 - \nu^2)y = 0 \quad (1.1)$$

is known as Bessel's equation.

If $\nu = 0$

The equation becomes as follows :

$$xy'' + y' + xy = 0 \quad (1.2)$$

is known as Bessel's equation of zero order.

Where the solution to Bessel's equation yields Bessel functions of the first and second kind as follows:

$$y = AJ_\nu(x) + BY_\nu(x) \quad (1.3)$$

where A and B are arbitrary constants. While Bessel functions are often presented in textbooks and tables in the form of integer order, i.e. $\nu = 0, 1, 2, \dots$, in fact they are defined for all real values of $-\infty < \nu < \infty$. is often encountered when solving boundary value problems, such as separable solutions to Laplace's equation or the Helmholtz equation, especially when working in cylindrical or spherical coordinates. The constant ν , determines the order of the Bessel functions found in the solution to Bessel's differential equation and can

take on any real numbered value. For cylindrical problems the order of the Bessel function is an integer value ($\nu = n$), while for spherical problems the order is of half integer value ($\nu = n + 1/2$). Since Bessel's differential equation is a second-order equation, there must be two linearly independent solutions. Typically the general solution is given as:

$$y = A J_\nu(x) + B Y_\nu(x)$$

where the special functions $J_\nu(x)$ and $Y_\nu(x)$ are:

1. Bessel functions of the first kind, $J_\nu(x)$ which are finite at $x = 0$ for all real values of ν (fig-2)
2. Bessel functions of the second kind, $Y_\nu(x)$, (also known as Weber or Neumann functions), which are singular at $x = 0$

The general solution of the equation (2) is as follows :

$$y = A J_0(x) + B Y_0(x) \quad (1.4)$$

$J_0(x)$ is called Bessel function of first kind of zero order, $Y_0(x)$ is called Bessel function of second kind of zero order.

The Bessel function of the first kind of order ν can be determined using an infinite power series expansion as follows :

$$J_\nu(x) = \sum_{r=0}^{\infty} \frac{(-1)^r \left(\frac{x}{2}\right)^{\nu+2r}}{r! \Gamma(\nu+r+1)}$$

$$= \frac{1}{\Gamma(1+\nu)} \left(\frac{x}{2}\right)^\nu \left\{ 1 - \frac{\left(\frac{x}{2}\right)^2}{1(1+\nu)} \left(1 - \frac{\left(\frac{x}{2}\right)^2}{2(2+\nu)} \left(1 - \frac{\left(\frac{x}{2}\right)^2}{3(3+\nu)} (1-\dots) \right) \right) \right\}$$

or by noting that $\Gamma(\nu+r+1) = (\nu+r)!$, we can write

$$J_\nu(x) = \sum_{r=0}^{\infty} \frac{(-1)^r \left(\frac{x}{2}\right)^{\nu+2r}}{r! (\nu+r)!} \quad (1.5)$$

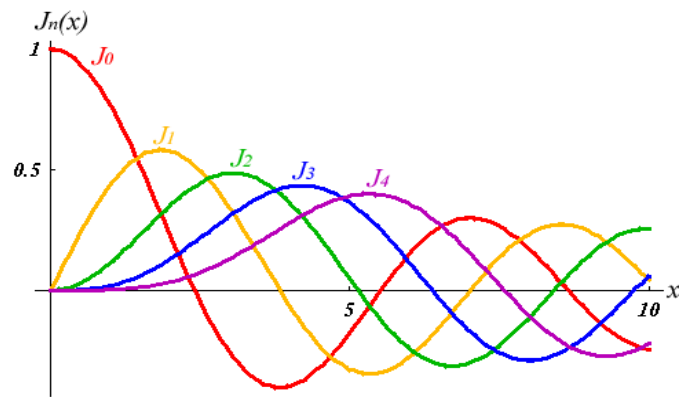


Fig-2: Bessel functions of the first kind, $J_n(x)$

If ν is an integer, the Bessel function of the first type are as follows :

$$J_{-\nu}(x) = \sum_{r=0}^{\infty} \frac{(-1)^r \left(\frac{x}{2}\right)^{-\nu+2r}}{r! \Gamma(-\nu+r+1)} \quad (1.6)$$

2. Generation of Heat:

The Photoacoustic effect follows the two-steps mechanism: i) the heat produced by the absorbed light radiation, ii) the generation of sound wave due to the medium thermal expansion. The first steps can be explained in details as following:

When the molecules are subjected to the laser beam, they absorb the photons and transform to the excited state. The mechanism of production of Heat through collision process can be understood by using two level model which is discussed as follow: In the excited state, the respective populations are N_b and $N - N_b$ of the excited and the ground energy levels E_b and E_a , respectively (Sigrist-

1994, Miklos, Hess-

2001, Miklos, Hess, Sneider, Kamm-1999)

Therefore, we can write the Rate equation for the excited level as follows:

$$\frac{dNb}{dt} = Nb' = (Na - Nb)\sigma\phi - \frac{Nb}{\tau} = (N - Nb)\sigma\phi - Nb\left(\sigma\phi + \frac{1}{\tau}\right) \left[\frac{1}{(\text{S.cm}^3)}\right] \quad (2.1)$$

Where ϕ is the incident photon flux which given by:

$$\phi(r, t) = \frac{E}{hf} g(r)\phi(t) \quad (2.2)$$

E is the pulse energy, g(r) is the normalized beam profile, h is Planck constant, σ is the absorption cross section of the transition, and τ is the global lifetime of the excited state, depending on the combined contributions from radiative and non-radiative deactivation processes which is define by following expression:

$$\frac{1}{\tau} = \frac{1}{\tau_r} + \frac{1}{\tau_{nr}} \quad (2.3)$$

Typically, in atmospheric conditions, the non-radiative lifetime τ_{nr} is much shorter than the radiative contribution τ_r (typically between 10^{-6} - 10^{-9} s and between 10^{-1} - 10^{-3} s (A.Hess, A.Sneider, J.Kamm, S.schafer-1999 [11]), so that we can approximate the total lifetime by its non-radiative component. The incident excitation rate $\sigma\phi$ is usually small enough. Therefore, we can consider that $Nb \ll N$ and then neglect it with respect to N. Hence the rate equation can be approximated by the following expression:

$$Nb'(r, t) = N\sigma\phi - \frac{Nb}{\tau} \left[\frac{1}{(\text{S.cm}^3)}\right] \quad (2.4)$$

In Photoacoustic approach the light source can either be modulated by an optical chopper in case of CW laser with emission frequency F_{mo} or pulsed laser with pulse repetition rate $F_p=1/T$ (T is pulse period= $2\pi/w_0$).

In case of modulated CW laser (square wave), the square pulse duration time τ_p is much greater than the non-radiative decay time τ_{nr} . Therefore, the steady state (i.e. $dNb/dt = 0$) is achieved directly after the start of square pulse and Nb(r, t) is rapidly decay to zero after the end of the pulse.

Based on equation No. 2.2 and 2.4 and the fact that the integration over the duration of one pulse is unity, we can write Nb(r, t) as follows:

$$Nb(r, t) = N\sigma g(r) \frac{E \tau_{nr}}{hf \tau_p} \quad (2.5)$$

In trace gas analysis, the absorption of light is very small. Therefore, the heat production rate H(r,t) is directly related to Nb(r, t) and given by following equations:

$$H(r, t) = \frac{Nb(r, t)hf}{\tau_{nr}} = H(r)H(t) = H(r) \sum_{n=-\infty}^{n=\infty} A_0 e^{inw_0 t} \quad (2.6)$$

$$\text{And} \quad H(r) = N\sigma g(r) \frac{E}{\tau_p} \quad (2.7)$$

In case of pulsed laser, the pulse duration time τ_p is much lesser than the non-radiative decay time τ_{nr} and the V-T energy which may transfer during the pulse is very small and does not play significant role. Therefore, collisional deactivation term in equation No. 2.4 can be eliminated and Nb'(r, t) is given by following equation:

$$Nb'(r, t \leq \tau_p) = N\sigma\phi \quad (2.8)$$

Assuming Nb(r, 0) = 0, the above equation can be integrated with the help of equations No.2.2 and 2.4. The result is expressed as:

$$Nb(r, \tau_p) = N\sigma g(r) \frac{E}{hf} \quad (2.9)$$

After the pulse, the first term in equation No.2.4 can be eliminated and the equation is given by:

$$Nb'(r, t \geq \tau_p) = -\frac{Nb(r, t)}{\tau_p} \quad (2.10)$$

So, using equation No.2.9, the solution can be written as:

$$Nb(r, t \geq \tau_p) = N \sigma g(r) \frac{E}{hf} e^{-t/\tau_{nr}} \quad (2.11)$$

Now the heat produced can be calculated using equation No. 2.6 and 2.11 and given by:

$$H(r, t) = H(r)H(t) = N \sigma g(r) \frac{E}{\tau_{nr}} \sum_{n=-\infty}^{n=\infty} A_n e^{inw_0 t} \quad (2.12)$$

3. Generation of Sound:

The inhomogeneous wave equation of the sound pressure in the lossless cylindrical resonator is well explained by different groups (Miklos, Lorincz-1989, Yehya & Chaudhary-2013, Miklos, Hess-2001, Miklos, Hess, Mohacs, Sneider, Kamm, Schafer -1999, Thomas-2006).

$$\frac{d^2 P(r, t)}{dt^2} - c^2 \nabla^2 P(r, t) = (\gamma - 1) \frac{dH(r, t)}{dt} \dots \dots (3.1)$$

Where c , γ and H are the sound velocity, the adiabatic coefficient of the gas and the heat density deposited in the gas by light absorption, respectively.

Because the sound velocity which is proportional to the gradient of $P(r)$ vanishes at the cell wall, the $P(r)$ must satisfy the boundary conditions of the vanishing gradient of $p(r)$ normal to the wall [9].

The solution of equation 3.1 is given by:

$$P(r, t) = C_0(t) + \sum_{n=0}^{\infty} C_n(t) P_n(r) \dots \dots (3.2)$$

Where $C_0(t)$, $C_n(t)$ are the eigen mode amplitude of corresponding sound wave, $C_n(t)$ is given by the Fourier series as :

$$C_n(t) = \sum_{n,m} A_{n,m} e^{imw_0 t} \dots \dots (3.3)$$

The dimensionless eigenmodes distribution of cylindrical resonator is the solution of the homogeneous wave equation and can be expressed as:

$$P_n(r, t) = P_n(r) e^{iw_n t} \dots \dots (3.4)$$

Where W_n is the resonance frequency of the cavity resonator, $P_n(r)$ is:

$$P_n(r) = P_{mnq}(r, \phi, z) = J_m(K_r r) \cos(K_z z) \left\{ \frac{\cos(m\phi)}{\sin(m\phi)} \right\} \dots \dots (3.5)$$

The amplitude (A_n) for modulated beam is:

$$A_n = \frac{iw_0(\gamma - 1)fn}{w_n^2 - w_0^2 + (iw_0 \frac{w_n}{Q})} \dots \dots (3.6)$$

and amplitude (A_n) for pulsed lasers is:

$$A_n = \frac{(\gamma - 1) L fn P_n(r_m) \alpha E}{V} \dots \dots (3.7)$$

Where fn is the overlap integral which describes the effect of overlapping between the pressure distribution of the n^{th} acoustic resonance frequency and the propagating laser beam divided by the normalized value of the n^{th} eigen mode as:

$$f_n = \frac{\int H(r) P_n(r) dv}{\int P_n^2(r) dv} \dots \dots (3.8)$$

The generated acoustic resonant modes inside the cylindrical cells can also be expressed as:

$$F_{mnq} = \frac{c}{2} \left(\left(\frac{\alpha_{mn}}{R} \right)^2 + \left(\frac{q}{l} \right)^2 \right)^{\frac{1}{2}} \dots \dots (3.9)$$

Where c is the sound velocity, α_{mn} is the n^{th} zero of the derivative of the m^{th} Bessel function at $r = R$, where R and l represent the radius and the length of the cylinder, respectively. The normal modes are

separated into longitudinal (q), radial (n) and azimuthal (m) modes.

Methods and Materials

The present study produces a modeling and simulation of the generated acoustic signal in a different resonance cavities. However, the paper divided to five sections as follow:

- First section deals with a modeling and simulation of a cylindrical cavities . we have started with one dimension then membranes as a two dimension of cylindrical cavity. Three dimension waves is the final result of this section. The study deals with three different size of cylindrical cavities.
- Second section deals with a modeling and simulation of a rectangular shapes . Three different size of rectangular shapes have been studied.

Results and Discussions:

First: PA waves in Cylindrical Cavity

Fig-3 shows the general form of cylindrical cavities. In our study we have used a three different size cavities as shown in table-23. Most of publications work on Photoacoustic spectroscopy have used the cylindrical cavity which refers to many reasons. Some of that reasons is foxing on losses and efficiency.

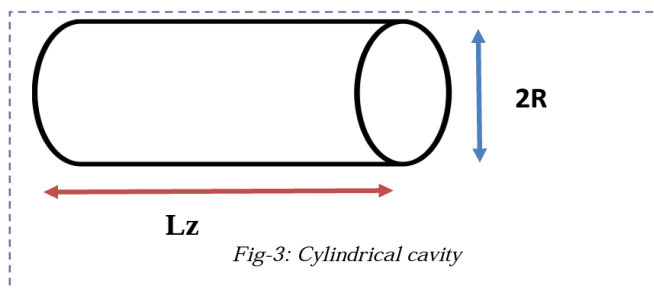


Fig-3: Cylindrical cavity

Table 1: Dimensions of three cylindrical cavities

3 cylindrical cavities			
	First cavity	Second cavity	Third cavity
Lz (cm)	10	50	1
R (cm)	4	10	0.3

A) Longitudinal Modes

In the longitudinal mode the indices $n=m=0$ and the resonance frequencies can be calculated by:

$$f_{00q} = qc/2l \dots \dots \dots (a.1)$$

Table 2: longitudinal frequencies for 3 cells(Hz)

K	Lz1=10cm	Lz2=50cm	Lz3=1cm
1	1715	343	17150
2	3430	686	34300
3	5145	1029	51450
4	6860	1372	68600
5	8575	1715	85750
6	10290	2058	102900
7	12005	2401	120050

The eigen functions of the longitudinal modes are given by the following expression:

$$P_n(r) = P_{00q}(z) = \cos(K_z z) \dots (a.2)$$

The simulation of the first four patterns of longitudinal frequency modes is shown in fig-1.2(a)

B) Radial & Azimuthal Modes

In the radial modes, the indices $m=q=0$ and the resonance frequencies are calculated by:

$$f = c\alpha'(0n)/2\pi \dots \dots \dots (b.1)$$

The eigen modes distribution is given by:

$$P_n(r) = P_{0n0}(r) = J_m(k_r r) \dots (b.2)$$

The simulation of the first four patterns of radial modes is shown in fig-1.2(b)

In the case of radial and azimuthal modes the indices $q=0$ and the resonance frequencies are calculated by using :

$$F_{mn0} = c\alpha'(mn)/2\pi r, \quad (n=1) \dots \dots (b.3)$$

and the eigen modes distribution is given by:

$$P_n(r) = P_{mn0}(r, \phi) = J_m(K_r r) \left\{ \frac{\cos(m\phi)}{\sin(m\phi)} \right\} \dots (b.4)$$

Table(4):Alfa for derivatives

N/ M	M=0	1	2	3
N=0	3.83170 6	7.015587	10.1734 7	13.3236 9
1	3.05423 7	6.706133	9.96946 8	13.1703 7
2	4.20118 9	8.015237	11.3459 2	14.5858 5
3	5.31755 3	9.282396	12.6819 1	15.9641 1

Table (5) Radial modes 3 cylindrical cavities ($c=34300\text{cm/s}$)

K	Rz1=4cm	Rz2=10cm	Rz3=0.3cm
			m

1	0	0	0
2	5229.327	2091.731	69724.35
3	9574.566	3829.826	127660.9
4	13884.32	5553.728	185124.3

Table (6) Azimuthal modes 3 cylindrical cavities ($c=34300\text{cm/s}$)

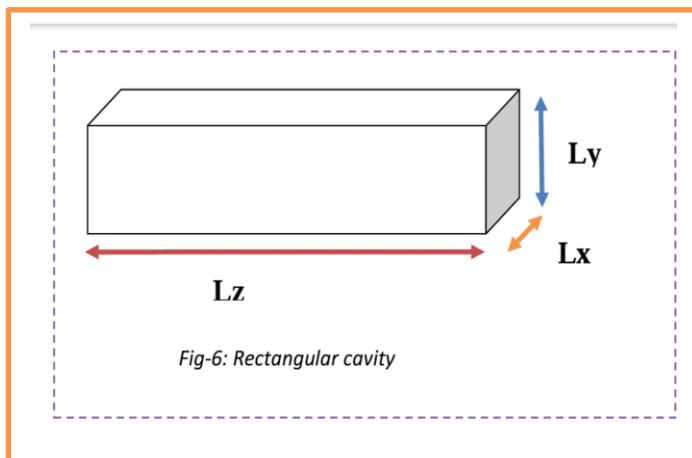
K	Rz1=4cm	Rz2=10cm	Rz3=0.3cm
			m
1	5229.327	2091.731	69724.35
2	7276.048	2910.419	97013.97
3	9152.174	3660.87	122029
4	10938.77	4375.509	145850.3

Second: PA waves in rectangular shapes:

The general solution (i.e. eigenvalues & eigenfunction) is:

$$F_{mnq} = A_{mnq} \sin\left(\frac{mx}{L_x}\right) \sin\left(\frac{my}{L_y}\right) \sin\left(\frac{mz}{L_z}\right) \dots \dots \dots (B.1)$$

$$F_{mnq} = \frac{c}{2} \sqrt{\left(\frac{m}{L_x}\right)^2 + \left(\frac{m}{L_y}\right)^2 + \left(\frac{m}{L_z}\right)^2} \dots \dots \dots (B.2)$$



3 Rectangular cavities			
	First cavity	Second cavity	Third cavity
Lx (cm)	5	10	3
Ly (cm)	10	10	3
Lz (cm)	50	30	20

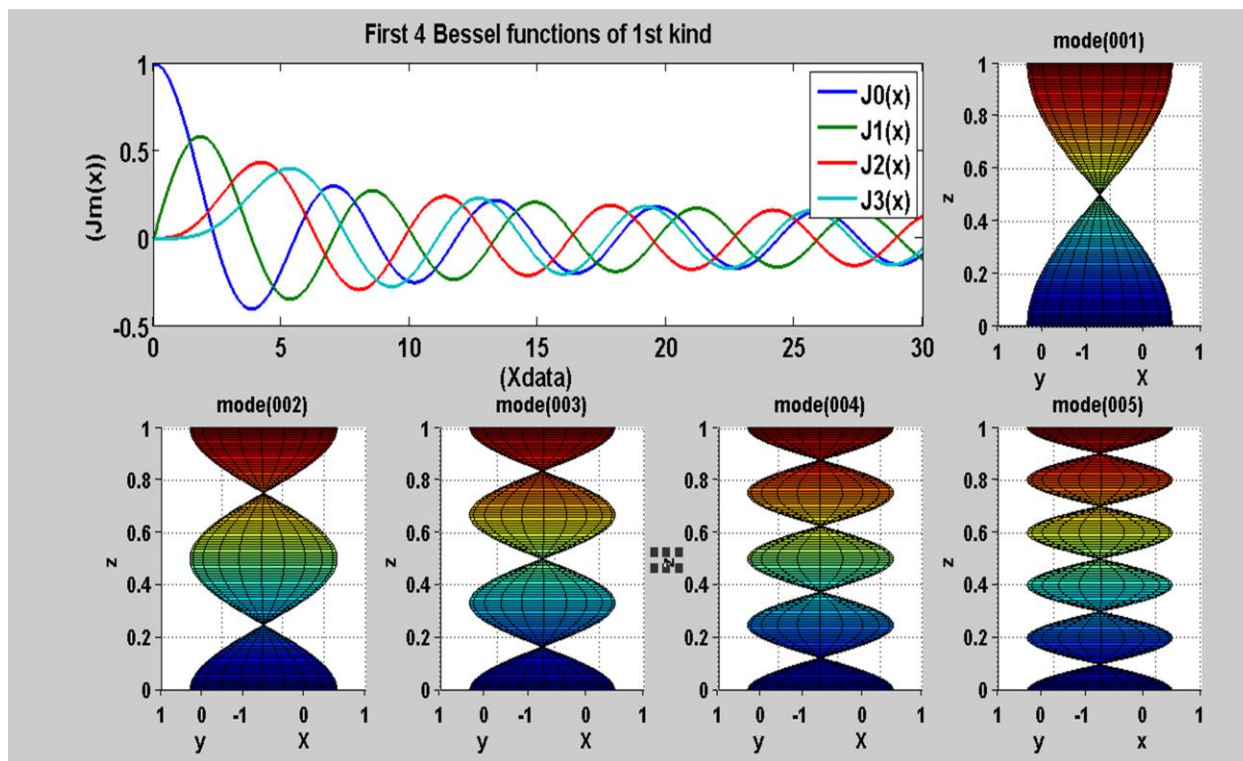


Fig. 4 the first longitudinal modes

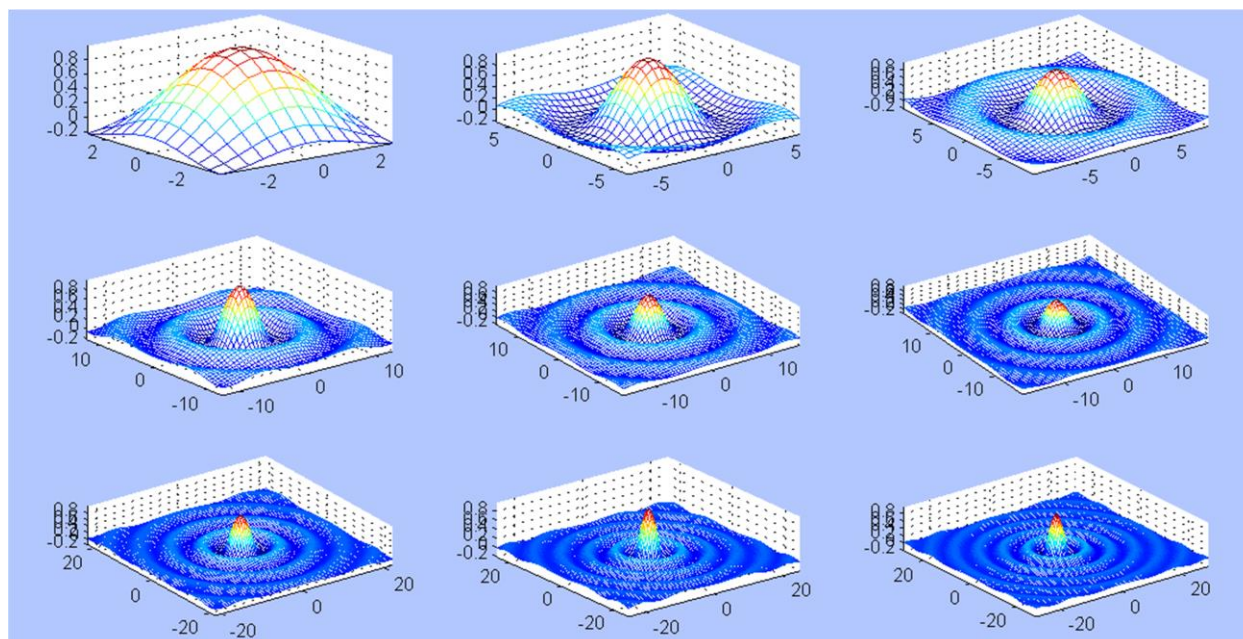


Fig- (5): The first patterns of radial modes

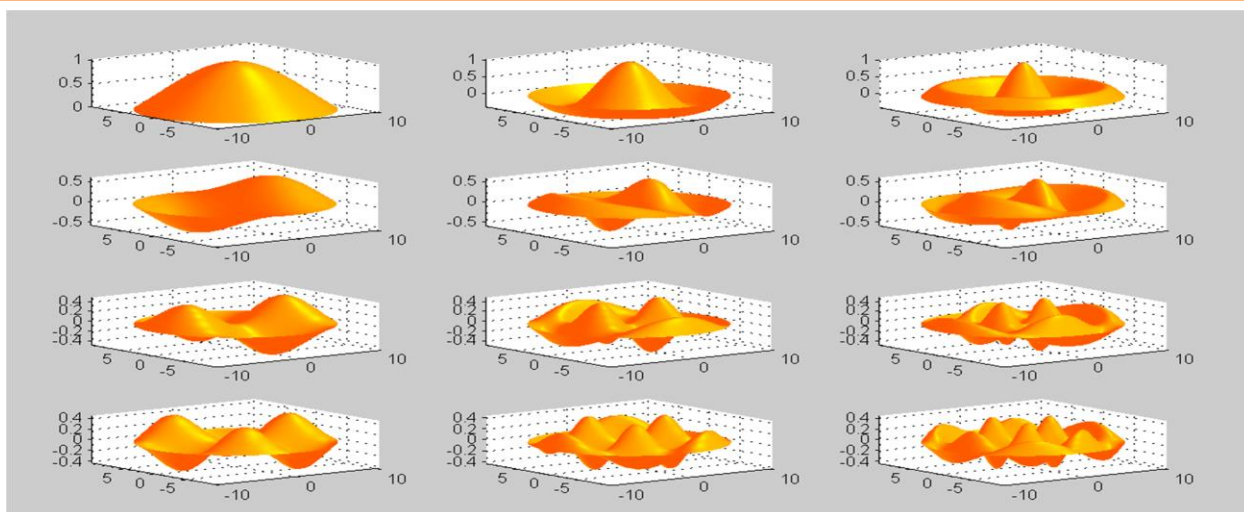


Figure (6): The first patterns of mixing (Azimuthal & Radial) modes

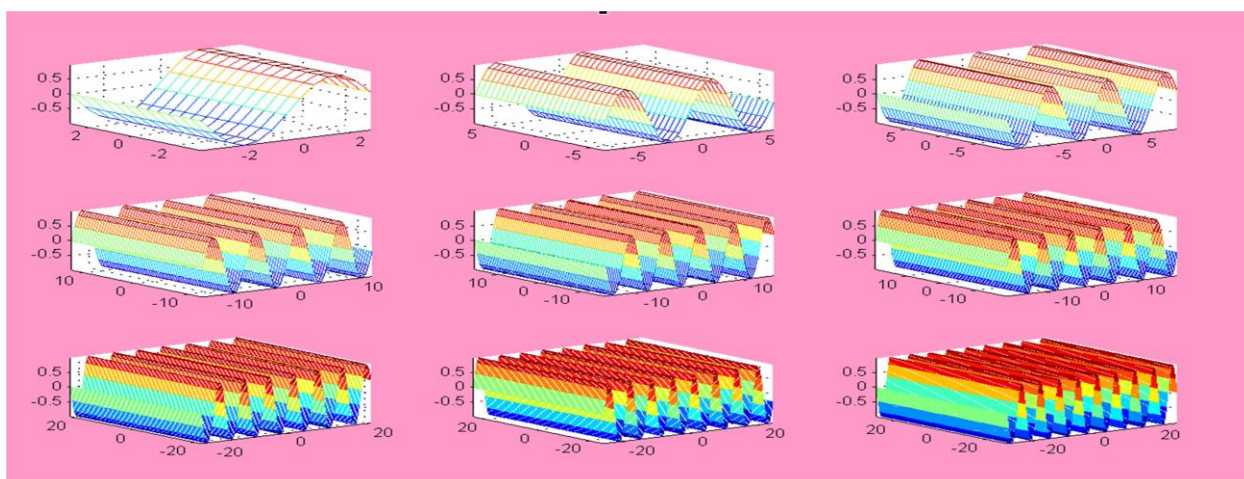


Fig- (7): Longitudinal modes in one dimension of rectangular shape

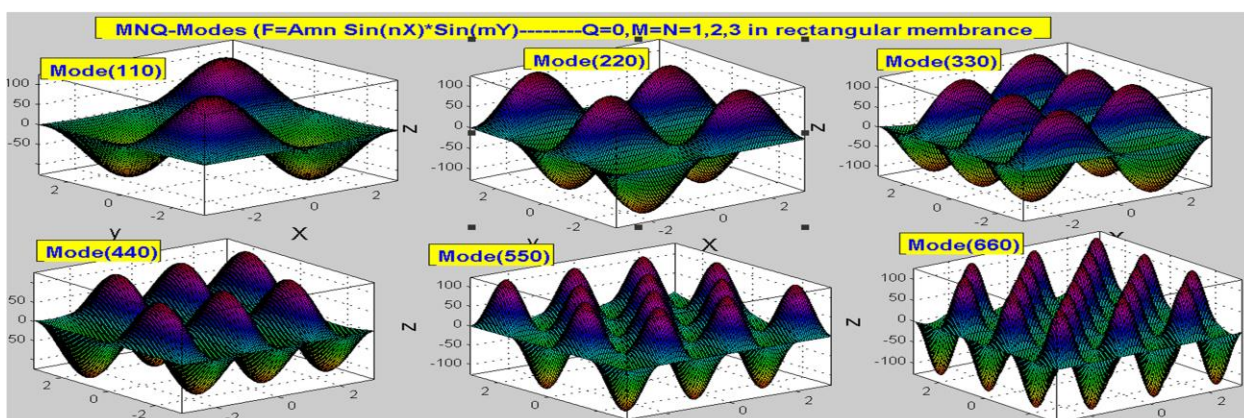


Fig- (8): Two dimension modes of rectangular shape

a) First Dimension

$$F_{m00} = A_{m00} \sin\left(\frac{mx}{L_x}\right) \dots\dots\dots (B.3)$$

(1-D means: F_{m00} or F_{0n0} or F_{00q})

$$F_{m00} = \frac{c}{2} \left(\frac{m}{L_x}\right) \dots\dots\dots (B.4)$$

<i>K</i>		<i>L_z1=50c m</i>	<i>L_z2=30c m</i>	<i>L_z3=20 cm</i>
1	343	571.7	857.5	
2	686	1143.3	1715	
3	1029	1715	2572.5	
4	1372	2286.7	3430	
5	1715	2858.3	4287.5	

b) Two dimensions

Eigenfunction & Eigenvalues:

$$F_{mn0} = A_{mn0} \sin\left(\frac{mx}{L_x}\right) \sin\left(\frac{my}{L_y}\right) \dots\dots\dots (B.5)$$

$$F_{mnq} = \frac{c}{2} \sqrt{\left(\frac{m}{L_x}\right)^2 + \left(\frac{n}{L_y}\right)^2} \dots\dots\dots (B.6)$$

<i>L_y(m) L_x(n)</i>	1	2	3	4	5
1	3835	4851	5184	7670	9236
2	7071	7670	8575	9702	1098
3	1.0432	1.0847	11505	1.2367	1.3395
4	1.3827	1.4142	1.4653	15339	1.6179
5	1.7236	1.7490	1.7905	1.8471	19174

Conclusions:

We have successfully simulated the generated photoacoustic signals inside different types of resonant cavities. The calculated values of

resonance frequencies for longitudinal, radial and azimuthal modes of the cavity resonators have been studied and used to simulate the higher order of their eigen functions. The study of surface losses indicates that the radial modes have minimum losses as compared to other modes. Similar study of rectangular cavities has been done. The study can be used as a basis to improve the cell design by introducing new types of special designing cells.

References:

- [1]. Kreuzer, L. B. J. (1971). *Appl. Phys.* (42) 2934.
- [2]. F. Yehya & A. K. Chaudhary. (2011). Designing and Modeling of Efficient Resonant photo Acoustic Sensors for Spectroscopic Applications. *Journal of Modern physics* (2) 200
- [3]. Sigrist, W. M. (1994) in *Air monitoring by spectroscopic techniques* (John Wiley and Sons, New York)
- A. G. Bell. (1880). *Am. J. Sci.* 5(118) 305.
- [4]. Tyndall, J. *Proc. Roy. Soc.* (31) 307
- [5]. W. C. Rontgen, *Ann.* (1881). *Phys. Chem.* (1) 155
- [6]. Tam, A. C. (1983). *Ultra sensitive laser spectroscopy* (Academic press, New York).
- [7]. Miklos, A. Lorincz, A. (1989). *Appl. Phys. B.* (48) 213.
- [8]. F. Yehya & A. K. Chaudhary, (2013). *Spectrochimica Acta Part A: Molecular and Biomolecular Spectroscopy.* (115) 544
- [9]. Miklos, A. Hess, P. (2001). *Rev. Sci. Instrum.* (72) 1937.
- [10]. Miklos, A. Hess, P. Mohacsi, A. Sneider, J. Kamm S. Schafer, S. (1999). "Photo Acoustic and Photo Thermal Phenomena," 10th International Conference, edited by I. F. Scudier and M. Bertolotti, AIP, Woodbury, New Jersey.
- [11]. Thomas, S. (2006). *Analytical & Bioanalytical Chem.* (384) 1071.